Development 128, 2929-2938 (2001)
Printed in Great Britain © The Company of Biologists Limited 2001
DEV2635

Prx1 and *Prx2* are upstream regulators of sonic hedgehog and control cell proliferation during mandibular arch morphogenesis

Derk ten Berge[1,*], Antje Brouwer[1], Jeroen Korving[1], Mark J. Reijnen[1], Estia J. van Raaij[1], Fons Verbeek[1], William Gaffield[2] and Frits Meijlink[1,‡]

[1]Hubrecht Laboratorium, Netherlands Institute for Developmental Biology, Uppsalalaan 8, 3584 CT Utrecht, The Netherlands
[2]Western Regional Research Center, ARS, USDA, Albany, CA 94710, USA
*Present address: Stanford University Medical Center, Beckman Center for Genetic and Molecular Medicine, 279 Campus Drive, Stanford, CA 94305-5323, USA
‡Author for correspondence (e-mail: frits@niob.knaw.nl)

Accepted 27 April 2001

SUMMARY

The *aristaless*-related homeobox genes *Prx1* and *Prx2* are required for correct skeletogenesis in many structures. Mice that lack both *Prx1* and *Prx2* functions display reduction or absence of skeletal elements in the skull, face, limbs and vertebral column. A striking phenotype is found in the lower jaw, which shows loss of midline structures, and the presence of a single, medially located incisor. We investigated development of the mandibular arch of *Prx1*$^{-/-}$*Prx2*$^{-/-}$ mutants to obtain insight into the molecular basis of the lower jaw abnormalities. We observed in mutant embryos a local decrease in proliferation of mandibular arch mesenchyme in a medial area. Interestingly, in the oral epithelium adjacent to this mesenchyme, sonic hedgehog (*Shh*) expression was strongly reduced, indicative of a function for Prx genes in indirect regulation of *Shh*. Wild-type embryos that were exposed to the hedgehog-pathway inhibitor, jervine, partially phenocopied the lower jaw defects of *Prx1*$^{-/-}$*Prx2*$^{-/-}$ mutants. In addition, this treatment led to loss of the mandibular incisors. We present a model that describes how loss of *Shh* expression in *Prx1*$^{-/-}$*Prx2*$^{-/-}$ mutants leads to abnormal morphogenesis of the mandibular arch.

Key words: Prx genes, Mandibular arch, Sonic hedgehog, Jervine, Mouse, Embryogenesis

INTRODUCTION

The mammalian head and neck region is, for a large part, derived from a series of pharyngeal arches. These structures contribute to many components of the face, jaws and ears, and to glands of head and neck. Each arch consists of a centrally located aortic arch artery, surrounded by mesenchyme derived from neural crest and paraxial mesoderm. Ectoderm covers the outside and pharyngeal endoderm lines the inner side. The first pharyngeal arch is the precursor of the jaws. The upper and lower jaws are derivatives from its maxillary and mandibular components, respectively.

Interactions between the surface epithelium and underlying mesenchyme are important in regulating growth and morphogenesis in the first pharyngeal arch (see, for example, Hall, 1980; Bee and Thorogood, 1980; Kollar and Mina, 1991). This epithelium has been shown to express many signaling factors, especially members of the Fgf, Bmp and hedgehog families (see Wall and Hogan, 1995 for *Bmp4*, *Bmp7* and *Fgf8*; Helms et al., 1997 for *Bmp2*, *Fgf8* and *Shh*; and Kettunen and Thesleff, 1998 for *Fgf8* and *Fgf9*). The functions of most of them in craniofacial development are poorly understood, which is due to either the lack of mutants or the presence of early phenotypes that interfere with later craniofacial development. It is likely that reciprocal interactions between epithelially and mesenchymally expressed factors guide patterning and outgrowth of the arch. An example of such interactions is the way in which *Fgf8* sets up oral-aboral polarity within the mandibular arch, and induces expression of the transcription factor genes *Lhx7* and *goosecoid* in the arch mesenchyme (Tucker et al., 1999). At a slightly later stage, Fgf8 performs another patterning function, as antagonistic interactions between Fgf8 and Bmp2 and Bmp4 induce *Pax9* expression in the mesenchyme, and thereby determine the sites of tooth formation in the mandibular arch (Neubüser et al., 1997). However, it remains poorly understood how the majority of genes expressed in the mandibular arch interact with each other, and how they control cell migration, proliferation and differentiation.

We are interested in the functions of a subset of the *aristaless*-related homeobox genes in morphogenesis of the skeleton (Meijlink et al., 1999), including *Prx1* and *Prx2*, *Alx3* and *Alx4*, and *Cart1*. *Prx1* and *Prx2* code for two highly similar proteins that share almost identical homeodomains and two other conserved domains, the aristaless-domain, and the prx-domain (Opstelten et al., 1991; Cserjesi et al., 1992; Kern et al., 1992; ten Berge et al., 1998b). *Prx1* loss-of-function mutants have skeletal abnormalities that are most severe at the lateral aspect of the skull, but milder defects are found in jaws, axial skeleton and limbs (Martin et al., 1995). While *Prx2* loss-

of-function mutants do not show any abnormalities, *Prx1*/*Prx2* double mutants show severe additional skeletal abnormalities in the skull, craniofacial region and limbs (ten Berge et al., 1998b). One of the most striking defects is found in the lower jaw, which is hypoplastic and contains no or only a single, median incisor.

We now demonstrate a genetic relationship between *Prx1* and *Prx2*, and the secreted signaling factor sonic hedgehog (Shh). Shh can act as a patterning gene in many different developmental settings. Examples are the limbs, where Shh produced by the zone of polarizing activity maintains anteroposterior polarity in the limb bud (Laufer et al., 1994; Niswander et al., 1994), and the neural tube, where Shh produced by the notochord induces the floorplate and sets up the dorsoventral axis (Echelard et al., 1993; Krauss et al., 1993; Chiang et al., 1996). Shh has also been shown to possess mitogenic activity. In the cerebellum, for example, Shh produced by Purkinje cells is responsible for expansion of granule cell precursor pools (Wechsler-Reya and Scott, 1999), and ectopic Shh promotes cell proliferation of retinal precursor cells (Jensen and Wallace, 1997).

Mice that lack a functional *Shh* gene demonstrate an almost complete absence of craniofacial skeletal elements, despite the presence and nearly normal appearance of the pharyngeal arches at E9.5 (Chiang et al., 1996). These authors do not describe further development of the arches. More insight into the role of hedgehog signaling in mandibular development has come from studies on the effects of the related teratogenic compounds jervine and cyclopamine. These alkaloids have been shown to inhibit all the hedgehog signaling pathways (Cooper et al., 1998; Incardona et al., 1998). Embryos exposed to jervine develop craniofacial abnormalities related to those found in *Shh* mutant embryos. The lower jaw of these embryos is severely reduced in size, often leading to loss of the incisors (Omnell et al., 1990). These data suggest that *Shh* is a major factor in stimulating outgrowth of the mandibular processes.

We now report results that suggest that Prx1 and Prx2 control cell proliferation and incisor positioning by regulating levels of *Shh* expression in the mandibular arch epithelium. We partially phenocopied the lower jaw defects of $Prx1^{-/-}Prx2^{-/-}$ mutants by inhibiting Shh signaling in the oral epithelium, using pharmacological and transgenic approaches. In addition, we found evidence that Shh exerts its effect on mandibular arch morphogenesis by regulating cell proliferation in specific areas of the mandibular arch mesenchyme. We have thus identified a novel molecular pathway that links the Prx genes to hedgehog signaling, in order to shape the developing mandibular arch.

MATERIALS AND METHODS

Animals

Prx2 mutant mice have been described previously (ten Berge et al., 1998b). *Prx1* mutant animals (Martin et al., 1995) were a kind gift from E. N. Olson (Dallas, TX).

Histological techniques and RNA in situ hybridization

Bone and cartilage staining, and preparation of sections, was conducted as described (ten Berge et al., 1998b). Radioactive RNA in situ hybridization was performed on paraffin wax-embedded sections (4-6 μm) as described (Leussink et al., 1995). The Alx3 probe has been described before (ten Berge et al., 1998a). Fgf8, Dlx2, Ptc and Shh probes were kind gifts from G. R. Martin (San Francisco, CA), J. Rubenstein (San Francisco, CA), U. Rüther (Hannover) and C. Tabin (Boston, MA), respectively.

Analysis of cell death and proliferation

Apoptotic cells were detected on 6 μm paraffin wax-embedded sections using the In Situ Cell Death Detection Kit (Boehringer Mannheim), according to the instructions of the manufacturer. In short, DNA ends were extended by terminal-deoxynucleotidyl transferase in presence of fluorescein-labeled dUTP. Incorporated fluorescein-labeled dUTP was detected using a Leica confocal laser-scanning microscope.

Cycling cells were detected by proliferating cell nuclear antigen (PCNA) immunohistochemistry. Paraffin sections (7 μm) were dewaxed, rehydrated and digested by pepsin. PCNA was detected by an HRP-conjugated mouse monoclonal anti-PCNA antibody (PC10; Santa Cruz Biotechnology).

Cell proliferation was assessed by measuring the extent of bromodeoxyuridine (BrdU) incorporation into cellular DNA. Pregnant mice were given intraperitoneal injections of BrdU (1 ml of 10 mM BrdU/100 g body weight) and embryos were isolated 1.5 hours later. Sections (4 μm) were prepared, and BrdU was detected using a fluorescein-labeled monoclonal anti-BrdU antibody (Roche), according to instructions of the manufacturer. The signal was enhanced using the Alexa Fluor 488 signal-amplification kit for fluorescein-conjugated probes (Molecular Probes). Sections were counterstained with the fluorophore TO-PRO-3 (Molecular Probes), which stains nucleic acids.

Each labeled section was scanned simultaneously for BrdU and TO-PRO-3 signals in two different channels using a Leica TCS NT confocal laser-scanning microscope. We assumed that an increase or decrease of cell proliferation would be reflected by a simultaneous increase or decrease of the number of BrdU-labeled nuclei in that area. A convolution with a Gaussian kernel (σ=16 pixels) was performed on both the BrdU and TO-PRO-3 images so that every point (pixel) in the resulting images represents a weighted average of its neighborhood. The convolution accomplishes that the signal in the circular area with radius of 1σ contributes for 39.3% to the new pixel value, a circle with radius of 2σ contributes for 86.5%, and a circle with radius of 3σ contributes for 99% to the new pixel value (the white horizontal line in the lower left corner of Fig. 3D indicates 3σ (48) pixels). After computing the ratio of BrdU to TO-PRO-3, a false color image was produced to facilitate the interpretation. The false colors ranged from yellow (low ratio of BrdU to TO-PRO-3) to dark red (high ratio of BrdU to TO-PRO-3; see scale bar in Fig. 3). In these false color images, an area in which the density of BrdU-labeled nuclei differs between mutant and control will also show a difference in color. A suitable value for σ was estimated by calculating false color images with a range of values for σ. The value for σ that best highlighted the differences between wild-type and mutant tissues was used to calculate the images shown in this report. A detailed description of this method will be published elsewhere (van Raaij et al., 2001).

Generation of transgenic animals

The *Ptc* overexpression construct p(BH1100)$_4$-*Ptc* was based on the construct p(BH1100)$_4$-*Alx3* (D. t. B., A. B. and F. M.). To make p(BH1100)$_4$-Alx3, a 1.8 kb *Eco*RI-*Ssp*I mouse *Alx3* cDNA fragment (ten Berge et al., 1998a) was cloned into the pSG5 expression vector (Stratagene). A *Stu*I-*Xba*I fragment containing the rabbit β-globin intron, the Alx3 cDNA and the SV40 polyadenylation signal was then isolated and cloned into p(BH1100)$_4$-*lacZ* (Charité et al., 1995), from which the *lacZ* and the polyadenylation signal were removed by *Bgl*II and *Not*I. This resulted in a construct in which *Alx3* was driven by the *Hoxb8* minimal promoter and four copies of the BH1100 enhancer. Most of the *Alx3* sequence was removed by *Bgl*II and *Sma*I, and replaced by a partially filled in *Spe*I-*Sal*I full-length Ptc cDNA

fragment (a kind gift from R. L. Johnson, Birmingham, AL). This resulted in the construct p(BH1100)$_4$-*Ptc*, in which the 45 bp most 5′ untranslated region of *Alx3* was left 5′ from the *Ptc* cDNA. Vector sequences were removed by *Sal*I digestion, and the construct injected into C57Bl/6 × CBA F2 zygotes. Embryos were recovered 14 days after the injected zygotes were transferred to pseudopregnant foster mothers, and stained for bone and cartilage as described (ten Berge et al., 1998b).

Jervine treatment of pregnant mice

Female A/J mice were mated with A/J males, and 10 mg jervine (400 mg/kg body weight) suspended in 400 µl water was administered orally at the indicated time points. Noon of the day the vaginal plug was detected was counted as E0.5. Fetuses were recovered on day 18 of gestation, decapitated, and stained for bone and cartilage as described (ten Berge et al., 1998b).

RESULTS

Abnormal tooth localization in the mandibular arch of *Prx1*$^{-/-}$*Prx2*$^{-/-}$ mutant embryos

The most striking phenotype in *Prx1*$^{-/-}$*Prx2*$^{-/-}$ mutants is loss of the mandibular incisors, or the occurrence of a single medial incisor. It is known that the mandibular incisors are positioned by antagonistic interactions between the epithelially produced signaling factors Fgf8 and Bmp2/4 (Neubüser et al., 1997). In the absence of Bmp2 or Bmp4, Fgf8 induces expression of the transcription factor gene *Pax9*, the earliest known mesenchymal marker for tooth induction, in the underlying mesenchyme. As a first step towards understanding the medial incisor phenotype, we therefore looked at the expression pattern of *Fgf8* in the mandibular arch of *Prx1*$^{-/-}$*Prx2*$^{-/-}$ mutants.

In E11.0 wild-type embryos, *Fgf8* was expressed in a lateral domain on both sides of the mandibular arch (Fig. 1A). In *Prx1*$^{-/-}$*Prx2*$^{-/-}$ mutant embryos, the *Fgf8* expression domains spread towards the midline of the mandibular arch and covered a medial area, forming a continuous large domain (Fig. 1B; see also ten Berge et al., 1998b). We have previously shown that *Pax9* is expressed underneath the medial domain of *Fgf8* expression, while *Bmp4* is absent from medial epithelium (ten Berge et al., 1998b). It is therefore likely that formation of the observed medial incisor in *Prx1*$^{-/-}$*Prx2*$^{-/-}$ mutants is the result of the medial expression of *Fgf8*.

We envisioned two mechanisms that might displace the mandibular domains of *Fgf8* expression towards the midline in *Prx1*$^{-/-}$*Prx2*$^{-/-}$ mutants. First, *Prx1/2* may regulate expression of *Fgf8* in the oral epithelium. As the expression patterns of *Prx1/2* and those of *Fgf8* do not overlap, this would have to occur via an indirect mechanism. Direct comparison of the *Prx1* and *Fgf8* expression domains in adjacent sections of E11 embryos, however, does not support a possible negative regulation of epithelial *Fgf8* by Prx activity in the adjoining mesenchyme as *Prx1* was expressed both in mesenchyme underneath *Fgf8*-positive and -negative epithelium (compare Fig. 1C with 1D; see also Kettunen and Thesleff, 1998). Alternatively, morphological changes of the mandibular processes may cause the *Fgf8*-expressing epithelium to be in a more medial position, without a direct influence on the regulation of *Fgf8* itself. The first morphological differences between mutant and wild-type mandibular arches became visible in sections of E10.5 embryos. The gap between the mandibular processes was wider in mutants than in wild-type embryos, and an excess of epithelium was found where the two processes fuse (compare Fig. 2B with 2C). In addition, this epithelium was often detached from the underlying mesenchyme (Fig. 2E; see also Fig. 1B). It is not clear, however, how these morphological changes relate to the changes in the *Fgf8* expression pattern, mainly owing to the lack of morphological landmarks in the mandibular arch at this stage. We therefore decided to use expression patterns of selected genes as substitutes for the morphological landmarks.

We chose to look at the expression of the homeobox genes *Dlx2* and *Alx3*. The expression patterns of these genes show distinct medial-lateral asymmetry in the mandibular arch (Qiu et al., 1997; ten Berge et al., 1998a). *Dlx2* is expressed complementarily to *Prx1* and *Prx2* (compare Fig. 2A with 2B). In contrast, the expression pattern of *Alx3* falls entirely within the expression domains of *Prx1* and *Prx2* in this region (compare Fig. 2A with 2D). The expression patterns were studied in two mutant and two wild-type embryos at E10.5. The changes described below were clearly visible throughout the mandibular arch of both mutant embryos.

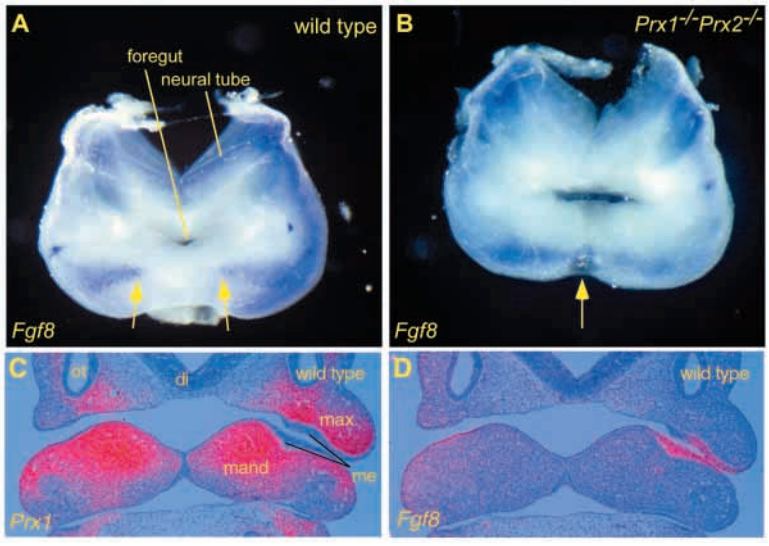

Fig. 1. *Fgf8* expression in the mandibular arch. (A,B) *Fgf8* whole-mount in situ hybridization on dissected mandibular arch region of E11 wild-type (A) and *Prx1*$^{-/-}$*Prx2*$^{-/-}$ (B) embryo, oral view. Dorsal side is upwards. Arrows in A indicate medial border of the *Fgf8* expression domain in the wild type. In the mutant, the *Fgf8* expression domain straddles the midline (arrow in B). Also visible in B is the distension at the midline (arrow), where the epithelium has detached from the mesenchyme. (C,D) Direct comparison of *Fgf8* and *Prx1* expression. Adjacent transversal sections through the mandibular arch area of E11 wild-type embryos were hybridized with radioactive Fgf8 and Prx1 probes. Double exposure of bright- and dark-field are shown; a red filter was used during darkfield photography. mand, mandibular arch mesenchyme; max, maxillary process mesenchyme.

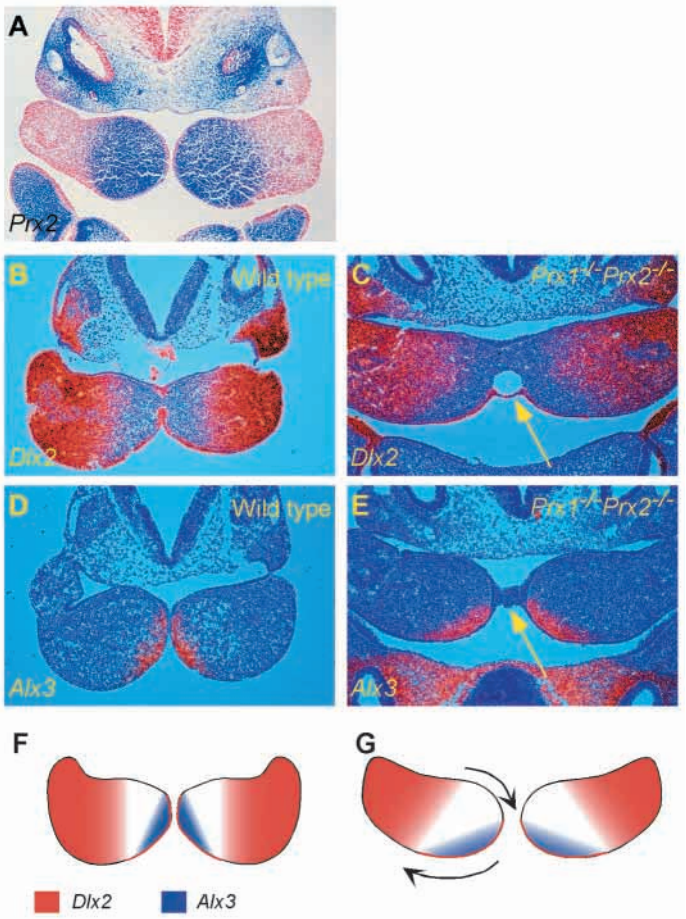

Fig. 2. Deformations and changes of patterning genes in mandibular arch of E10.5 embryos. (A) *Prx2* expression in *Prx2*$^{+/-}$ embryo visualized by β-galactosidase staining (blue). In situ hybridization with Dlx2 (B,C) and Alx3 (D,E) probes on nearby sections of wild-type (B,D) and *Prx1*$^{-/-}$*Prx2*$^{-/-}$ (C,E) embryos. Expression is indicated in red. Owing to small differences in stage and orientation of embryos, sections at comparable levels do differ in shape and size. (F,G) The shift of the expression domains of *Dlx2* and *Alx3* in *Prx1*$^{-/-}$*Prx2*$^{-/-}$ embryos (G) compared with wild-type embryos (F). Arrows in C,E indicate abnormal epithelium. Dorsal is upwards.

Dlx2 expression in wild-type embryos was found laterally in the mesenchyme, with a sharp expression border that ran vertically from oral to aboral (Fig. 2B). In *Prx1*$^{-/-}$*Prx2*$^{-/-}$ mutant embryos, the expression border was slightly rotated and ran obliquely. The expression border at the aboral side was positioned more laterally than in the wild type, while at the oral side it was more medially located (Fig. 2C). In addition, expression in the epithelium was shifted in an oral-to-aboral direction (compare Fig. 2B with 2C). *Alx3* is normally expressed medially in the mesenchyme of the mandibular processes (Fig. 2D). In the *Prx1*$^{-/-}$*Prx2*$^{-/-}$ mutant, this expression domain was shifted towards a more lateral aboral position (Fig. 2E). The changes in the patterns are summarized in schematic drawings (Fig. 2F,G), which suggest that the medial domains of the mutant mandibular processes have undergone a rotating movement, with the oral region moving in a medial direction, and the aboral region in a lateral direction. The oral expression pattern of *Fgf8* has undergone a similar type of movement in a medial direction (Fig. 1). These data suggest that the medial shift of the *Fgf8* expression pattern was indeed due to a change in morphology of the mandibular process.

We have used gene expression patterns as morphological landmarks in mutant embryos, assuming that these patterns have not changed as a result of abnormal regulation. We think that this is a reasonable assumption because, first, the expression levels of *Dlx2* and *Alx3* have not changed, and, second, the expression domains of *Dlx2* and *Fgf8* do not overlap with those of *Prx1* or *Prx2*, making direct regulation unlikely. This does not exclude the possibility of indirect regulation, but the factor(s) that mediate this regulation should then act on the entire mesenchymal domain, as well as on the epithelium. Moreover, *Dlx2*, *Alx3* and *Fgf8* should then all be (indirect) target genes of *Prx1* and *Prx2*. A change of the expression patterns due to a deformation of the mandibular arch is a simpler and more plausible explanation for the coherent shifts in expression domains of these three genes.

Local cell proliferation defects in *Prx1*$^{-/-}$*Prx2*$^{-/-}$ mandibular arch

Abnormal morphogenesis can be the result of inappropriate cell migration, differentiation, or proliferation. The presence of a *lacZ*-coding region in the mutated *Prx2* allele allowed us to analyze the distribution of cells that normally would have expressed *Prx2*. This analysis did not provide evidence for abnormal migratory behavior of these cells. We therefore proceeded to investigate cell proliferation and differentiation in *Prx1*$^{-/-}$*Prx2*$^{-/-}$ mutants.

Defects in expansion of precursor cell populations can arise as a result of abnormal cell death, premature differentiation and exit from the cell cycle, or reduced mitogenesis. Cell death analysis showed apoptotic cells in distinct patterns in both wild-type and mutant mandibular arch at E10.5 and E11.5 (not shown). No significant difference could be found between wild-type and mutant embryos, indicating that cell death is not a cause of abnormal morphology.

Cell proliferation in the mandibular arch was assessed by both PCNA immunohistochemistry and in vivo BrdU pulse labeling. PCNA is a marker for cycling cells, and cells negative for PCNA have presumably entered rest phase (Mathews et al., 1984). Almost all cells in the E10.5 and E11.5 mandibular arch were positive for the anti-PCNA antibody, and no significant differences were found between wild-type and mutant embryos (data not shown). This indicates that the cause of any growth difference in the mutant mandibular arch is not at the level of cells entering or leaving the cell cycle. In addition, the expression patterns of *Fgf8*, *Alx3* and *Dlx2* (Figs 1, 2) suggest that overall patterning of the mandibular arch around E10.5 is relatively normal in *Prx1*$^{-/-}$*Prx2*$^{-/-}$ mutants, and do not indicate inappropriate differentiation of cells.

Even if the fraction of cells that cycle is unchanged, it is still possible that other parameters pertaining to the cell cycle have changed. If the cycle had slowed down, this would not be detected by PCNA analysis but it should become apparent by measuring BrdU incorporation. When we assessed mitogenic activity using in vivo BrdU labeling, we did observe a local difference in cell proliferation in the E10.5 mutant mandibular arch. BrdU incorporation was detected on sections using fluorescently labeled antibodies. To identify domains with

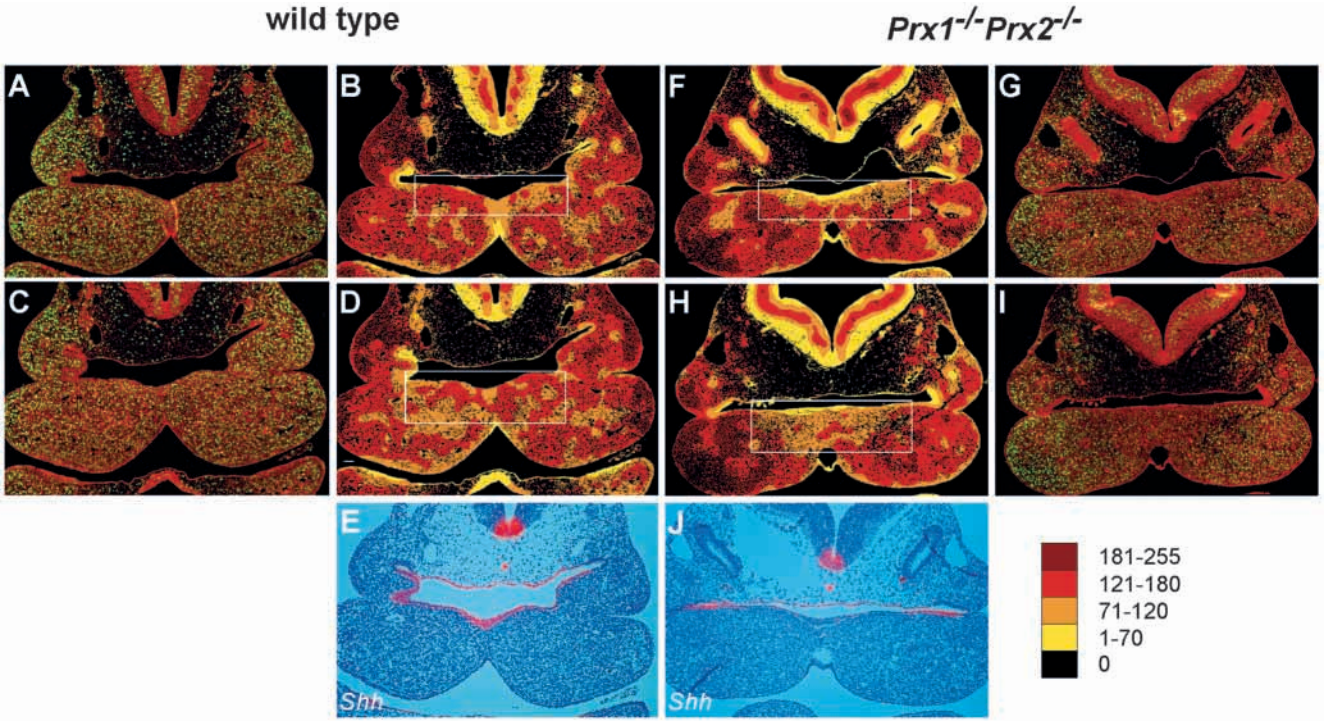

Fig. 3. Detection of BrdU labeling in transverse sections of the mandibular arch of E10.5 wild-type (A,C) and *Prx1*$^{-/-}$*Prx2*$^{-/-}$ mutant (G,I) embryos. (B,D,F,H) False color representations of A,C,G,I (respectively) to aid in interpretation (see Materials and Methods section). The strength of labeling is indicated by a color series ranging from yellow (weakest) to dark red (strongest), corresponding to ranges of arbitrary units as indicated. Boxed areas in the false color figures indicate areas in which the mutant shows reduced labeling compared with the wild type. White horizontal line in left lower corner of D indicates 48 pixels. (E,J) Nearby sections from wild-type (E) and *Prx1*$^{-/-}$*Prx2*$^{-/-}$ (J) embryos showing expression of *Shh* in red. Dorsal is upwards.

similar average labeling, and to highlight differences between wild-type and *Prx1*$^{-/-}$*Prx2*$^{-/-}$ embryos, images were quantitatively analyzed, and the results were visualized as false color images (see Materials and Methods section). We analyzed six wild-type and six mutant embryos. In wild-type, as well as mutant embryos, we identified distinct domains in the mandibular arch that were labeled either strongly or weakly with the anti-BrdU antibody (Fig. 3). In wild-type embryos, labeling was strong in the central core of the arch. This domain extended into the region underneath the oral and aboral epithelium. Weak labeling was observed in the medial domain of the mandibular arch (Fig. 3A-D). Significantly, in all *Prx1*$^{-/-}$*Prx2*$^{-/-}$ mutant embryos tested, we found BrdU incorporation to be lower in the region underneath the oral epithelium, and the medially located weakly labeled domain had extended laterally underneath the oral epithelium (Fig. 3F-I). In contrast, slight variations in BrdU labeling seen in the aboral compartment of the mandibular arch and in regions that are more proximal were not reproducible. This reduction of BrdU labeling in the mesenchyme underneath the oral epithelium of *Prx1*$^{-/-}$*Prx2*$^{-/-}$ mutants indicates that the rate of mitotic activity in this area was reduced.

Sonic hedgehog is downregulated in mandibular arch epithelium of *Prx1*$^{-/-}$*Prx2*$^{-/-}$ mutants

The signaling molecule Sonic hedgehog (Shh) is well known for its role in many developmental processes. It has been shown to act as a morphogen, as well as to possess mitogenic activity, and has been implicated in midline specification in the spinal cord and the face (Ericson et al., 1995; Chiang et al., 1996; Roessler et al., 1996). The proliferation abnormalities and midline nature of the mandibular defects in Prx mutants prompted us therefore to investigate the expression pattern of *Shh*.

The expression pattern of *Shh* was actually changed in the mutant mandibular processes. In E10.5 wild-type embryos, *Shh* was expressed in lateral and medial domains in the oral epithelium of the mandibular processes whereas in *Prx1*$^{-/-}$*Prx2*$^{-/-}$ mutants the level of *Shh* expression in the medial domain was considerably reduced. This was observed in six different mutants and is shown in Fig. 3E,J to allow direct comparison with the localization of the area of diminished proliferation. Strikingly, the epithelium where *Shh* is downregulated abuts the mesenchyme where lower BrdU incorporation was seen. To further explore the effect on *Shh* expression we analyzed a series of wild-type and mutant embryos of stages from E9.5 to E10.5, as illustrated in Fig. 4. Expression was normal at E9.5 (not shown) and in a slightly more advanced embryo with 26-27 somites (Fig. 4A,B). In embryos with 30-31 somite embryos (about E10), medial epithelial *Shh* was noticeably lower (Fig. 4C,D), but still higher than at the maximum degree of downregulation seen at E10.5.

The observation that the reduction of mesenchymal proliferation in *Prx1*$^{-/-}$*Prx2*$^{-/-}$ mutants was located underneath the oral epithelium that showed reduced *Shh* expression (compare Fig. 3A-E with 3F-J) suggests that Shh in the epithelium has a role in growth regulation in the oral mesenchyme. The reduction of *Shh* expression in

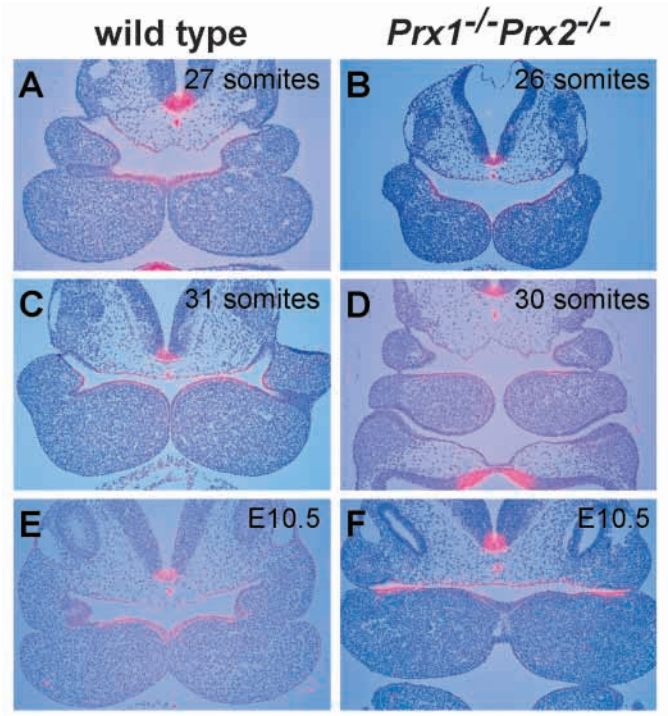

Fig. 4. Decrease of *Shh* expression in *Prx* mutants in time. Radioactive hybridization on cross-sections of embryos of various stages as indicated. (A,C,E) Wild type; (B,D,F) *Prx1*$^{-/-}$*Prx2*$^{-/-}$ mutant.

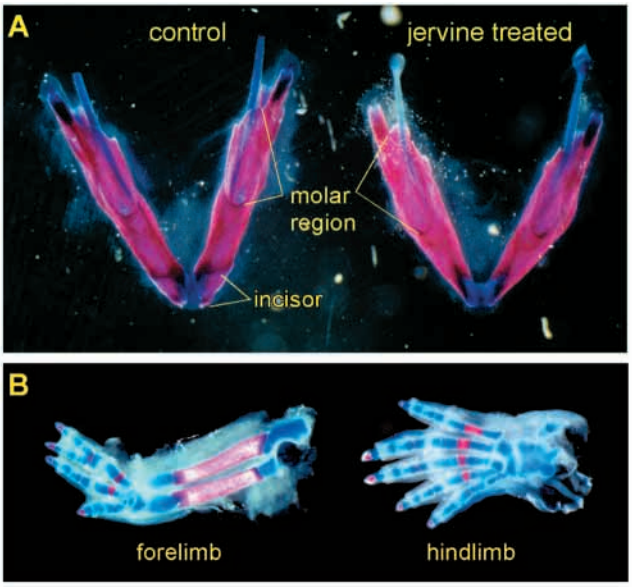

Fig. 5. Effects of jervine on lower jaw and limb development. (A) Exposure of embryos to jervine at E9.5 results in truncation of the distal lower jaw and loss of the incisors. Proximal is upwards. (B) Jervine exposure at E9.5 induces oligosyndactyly in the forelimb (left), but mainly carpal fusions in the hindlimb (right).

Prx1$^{-/-}$*Prx2*$^{-/-}$ mutants may therefore be causative for the observed lower jaw abnormalities. To test this hypothesis, we designed two independent ways to inhibit *Shh* signaling in the mandibular arch. These should lead to lower-jaw phenotypes similar to those observed in *Prx1*$^{-/-}$*Prx2*$^{-/-}$ mutants.

Interfering with Shh signaling leads to mandibular abnormalities and loss of incisors

The veratrum alkaloids cyclopamine and jervine have been demonstrated to inhibit transduction of the Shh signal (Cooper et al., 1998; Incardona et al., 1998). We therefore studied the effect of jervine treatment on development of the mandible.

Jervine was administered to pregnant mice at various stages of pregnancy: at early day 9.5 of gestation, late day 9.5 of gestation and early day 10.5 of gestation. We chose these stages because they surround the stage at which the downregulation of *Shh* in *Prx1*$^{-/-}$*Prx2*$^{-/-}$ mutant embryos takes place. To verify that jervine did in fact inhibit Shh signaling in the embryo, we looked at the expression of a direct target of Shh signaling, *Patched* (*Ptc*; Goodrich et al., 1996). Embryos that were isolated 4 hours after jervine treatment at early day 9.5 of gestation displayed significantly reduced *Ptc* expression in the branchial arch mesenchyme, although this downregulation was not complete (not shown). This observation demonstrates that the applied doses of jervine were sufficient to cause a significant inhibition of Shh signaling within 4 hours of administration.

Embryos treated with jervine were isolated at E18.5, stained for bone and cartilage, and inspected for skeletal malformations. Embryos treated at early E10.5 displayed mild oligosyndactyly, suggesting that the jervine had been effective in inhibiting Shh signaling. However, no or very minor mandibular abnormalities were found (not shown), indicating that development of the mandible is not dependent on hedgehog signaling around E10.5. In contrast, embryos treated at early and late E9.5 displayed a clear reduction in size of the lower jaw (Fig. 5A). The proximal part of the mandible was relatively normal, and the molar area seemed unaffected. The distal part was, however, strongly reduced, and the incisors were absent (Fig. 5A). The teratogenic effect of jervine was not fully penetrant: from four litters treated with jervine at E9.5, two litters showed only mild abnormalities (not shown), while the other two litters showed the phenotypes described above. Within litters, the variability of the phenotypes was low.

By comparing abnormalities in fore- and hindlimbs of jervine-treated fetuses, we could estimate a time frame within which the jervine is active in the embryo. Fetuses exposed to jervine at E9.5 showed severe oligosyndactyly in the forelimbs, while mainly fusions of carpal bones were found in the hindlimbs (Fig. 5B). At E10.0, a combination of moderate fore- and hindlimb oligosyndactyly was found (not shown). These phenotypes indicate that jervine administered at E9.5 is active during development of the forelimb autopod, but is cleared from the embryo's system before development of the hindlimb autopod starts. As the hindlimbs lag behind in development approx. 0.5-1.0 day compared with the forelimbs, these phenotypes indicate that jervine is active in the embryo for less than 1 day.

Our results indicate that the downregulation of *Shh* in *Prx1*$^{-/-}$*Prx2*$^{-/-}$ mutants is responsible for at least part of the mandibular phenotype of these animals. Jervine-induced defects are concentrated in the distal lower jaw and the incisors, as in *Prx1*$^{-/-}$*Prx2*$^{-/-}$ mutants. However, jervine treatment does not seem to induce the medial dislocations of oral structures

seen in *Prx1*$^{-/-}$*Prx2*$^{-/-}$ mutants. Therefore, a medial shift of the *Fgf8* and *Pax9* expression domains, as seen in *Prx1*$^{-/-}$*Prx2*$^{-/-}$ mutants, was not expected. We did, however, envisage a lower level of expression of these genes. In situ analysis of E11.0 embryos from mothers treated at E9.5 with jervine revealed normal *Fgf8* and *Pax9* expression patterns both in location and, to our surprise, in level (not shown).

The use of pharmacological agents is often accompanied by nonspecific effects, caused by interference of the compound with other processes. However, the defects that we observed were specific for and limited to regions known to depend on hedgehog signaling. To further confirm that the mandibular abnormalities of jervine-treated fetuses were due to interference with hedgehog signaling, we used as an alternative a transgenic approach to inhibit hedgehog signaling specifically in the first pharyngeal arch. This was done by overexpression of the hedgehog receptor Ptc in the neural crest-derived mesenchyme of the first pharyngeal arch. Ptc inhibits the downstream factor smoothened (Smo), and this inhibition is relieved by binding of Shh to Ptc, leading to downstream signaling and target gene activation. Overexpression of *Ptc* therefore leads to constitutive inhibition of Smo and loss of responsiveness to hedgehog signaling, as has been shown in *Drosophila* and mice (Johnson et al., 1995; Goodrich et al., 1999).

In the transgene construct, *Ptc* was driven by a enhancer/promoter that is expressed in mesenchyme of the mandibular arch, in addition to a typical *Hox* expression pattern in mesoderm and neural tube of the trunk. This construct consists of four copies of a 1.1 kb *Bam*HI-*Hin*dIII fragment named BH1100 and located 3.6 kb upstream from the mouse *Hoxb8* transcription start site, linked to a 1 kb fragment containing the transcription initiation site. Embryos transgenic for a construct in which this promoter is linked to *lacZ* display β-galactosidase activity in most of the neural crest-derived mesenchyme of the mandibular arch. This domain includes, but is much larger than the expression domain of *Ptc* in normal embryos (see Charité et al., 1995 for further information). Transgenic embryos were isolated at E14.5 for phenotypic analysis. Mutant embryos developed fairly normally, and showed no craniofacial abnormalities outside the domains of expression of the transgene construct. The lower jaw was however considerably shorter and narrower. A typical example of this phenotype is shown in Fig. 6B and compared with wild-type (Fig. 6A) and Prx mutant (Fig. 6C,D) embryos to demonstrate the similarity in phenotype. In frontal sections, however, it could be seen that there was no medial shift of the incisor buds (not shown). These jaw phenotypes resemble those of jervine-treated embryos, although of lesser severity. The relatively mild phenotypes might be a result of low level expression from the *Hoxb8* promoter/enhancer combination that was used. These observations confirm that the phenotypes caused by jervine treatment are a result of the compound's action on the hedgehog pathway.

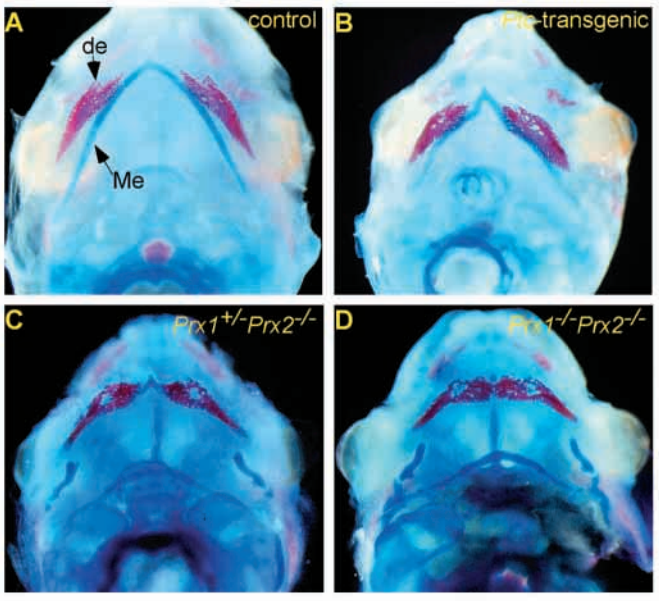

Fig. 6. Reduction of lower jaw in *Ptc* transgenic embryos. E14.5 *Ptc* transgenic embryo (B) shows a shorter jaw than a wild-type example (A). (C,D) For comparison, skeletal staining of *Prx* mutant embryos are included to reveal similarities in mandibular phenotype. de, dentary; Me, Meckel's cartilage.

DISCUSSION

In this report, we present results of the cellular and molecular analysis of mandibular arch development in *Prx1*$^{-/-}$*Prx2*$^{-/-}$ mutant embryos. We reported previously that these mutants develop a very short and narrow lower jaw, in addition to other skeletal defects. Part of the lower jaw phenotype is a loss of midline structures. With progressive loss of Prx genes, the incisors shift towards the midline, to such an extent that usually only a single, medial incisor is observed in *Prx1*$^{-/-}$*Prx2*$^{-/-}$ mutants. Structures normally located between the incisors are lost. Occasionally, however, in a strong expression of the phenotype, both incisors are lost (ten Berge et al., 1998b).

Fgf8 has been shown to determine the position of the teeth by inducing *Pax9* in the underlying mesenchyme (Neubüser et al., 1997). We show here that, at E11.0, the normal domain of *Fgf8* expression in oral epithelium has shifted towards the medial tips of the mandibular processes. *Pax9* expression is induced in the mesenchyme underneath the *Fgf8* expressing epithelium. Upon fusion of the mandibular processes, these medial domains of *Pax9* coalesce into a single medial domain that supposedly leads to development of a single medial incisor (ten Berge et al., 1998b).

Alx3 and *Dlx2* also demonstrated a medial shift of their expression domains in the oral part of the mandibular arch. In the aboral part, however, we show that their expression domains had shifted in the lateral direction. We do not think that *Prx1* or *Prx2* directly regulate *Fgf8*, *Alx3* or *Dlx2*, because their expression levels have not changed. In addition, the expression patterns of *Fgf8* and *Dlx2* show little overlap with those of *Prx1* or *Prx2* (see Figs 1C,D, 2A,B; Kettunen and Thesleff, 1998). Rather, we believe that these results demonstrate that morphogenesis of the mandibular arch in *Prx1*$^{-/-}$*Prx2*$^{-/-}$ mutants occurs abnormally, such that oral regions develop more medially than in wild-type embryos, while aboral regions develop more laterally. The resulting change in shape therefore appears causative for the medial shift of the incisors in *Prx1*$^{-/-}$*Prx2*$^{-/-}$ mutants.

Prx1 and *Prx2* maintain *Shh* expression in oral epithelium

Expression of *Shh* in oral epithelium of *Prx1*$^{-/-}$*Prx2*$^{-/-}$ mutants was downregulated from late E9.5 (30 somites) onwards, whereas it was expressed at a normal level at earlier stages. This indicates that *Prx1* and *Prx2* are not required to induce *Shh*, but to maintain appropriate expression levels in the oral epithelium. As *Prx1* and *Prx2* are not expressed in the oral epithelium, but only in the underlying mesenchyme, they can not directly regulate *Shh*. We therefore propose that the Prx genes regulate the production of a mesenchymal signal that maintains *Shh* expression in the overlying epithelium.

Shh is required for mandibular outgrowth and initiating incisor development

Failure to maintain appropriate levels of *Shh* expression in oral epithelium may be causative for the mandibular abnormalities of *Prx1*$^{-/-}$*Prx2*$^{-/-}$ mutants. A very good way to test this hypothesis would have been to try to rescue the phenotype by local expression of Shh. This requires either a promoter that can deliver, in transgenic experiments, Shh to the medial epithelial domain, or a culture system that is reliable enough to reproduce the mandibular defects in vitro. Because of the technical problems associated with such a method, we chose two other approaches to test our hypothesis, one pharmacological and one transgenic.

Treatment of pregnant mice with the hedgehog inhibitor jervine induced jaw defects in the embryos similar to those found in *Prx1*$^{-/-}$*Prx2*$^{-/-}$ embryos. The distal part of the jaw was reduced in size, and both incisors were absent. Susceptibility for jaw defects was highest when treatment took place around E9.5. Based on autopod phenotypes, we could estimate that the jervine was active in the embryo for, at most, 1 day. This timecourse of jervine action indicates that downregulation of *Shh* in *Prx1*$^{-/-}$*Prx2*$^{-/-}$ mutants occurred during a stage in which the mandibular arch is highly dependent on Shh for normal development. Furthermore, the first visible sign of incisor development is at E11.5, and it is remarkable that jervine inhibits incisor development 1.5-2.0 days in advance of that. We confirmed the specificity of the jervine effect by also inhibiting hedgehog signaling in a transgenic manner. We overexpressed *Ptc* in the neural crest-derived mesenchyme of the first pharyngeal arch in transgenic embryos, and showed that this results in shortening and narrowing of the lower jaw. The effect on mandibular outgrowth was not as severe as in *Prx1*$^{-/-}$*Prx2*$^{-/-}$ mutants or in fetuses exposed to jervine, and we think it likely that the *Hoxb8* enhancer/promoter combination that we used was not sufficiently strong to inhibit all hedgehog signaling. Nevertheless, these malformations support the notion that a hedgehog signal is required in the mesenchyme for correct outgrowth of the mandibular arch.

A distinct difference between *Prx1*$^{-/-}$*Prx2*$^{-/-}$ mutants and jervine-exposed or *Ptc* transgenic embryos is the absence of midline deletions in the lower jaw of jervine-exposed embryos. Although the incisors were deleted in jervine-exposed fetuses, there was no fusion between the dentaries, as in *Prx1*$^{-/-}$*Prx2*$^{-/-}$ mutants. This may suggest that lack of Shh is only partially responsible for the *Prx1*$^{-/-}$*Prx2*$^{-/-}$ jaw phenotype. However, because it is likely that the jervine causes a global inhibition of hedgehog signaling, an alternative explanation is that jervine-induced inhibition of Shh signaling laterally in the mandibular arch has additional consequences for morphogenesis that prevent the midline shifting of oral structures observed in *Prx1*$^{-/-}$*Prx2*$^{-/-}$ embryos. The same reasoning can be used for the *Ptc* transgenic embryos, as *Ptc* was overexpressed throughout the mandibular mesenchyme in these animals. It remains currently unclear by which molecular mechanism reduced hedgehog signaling leads to the mandibular phenotype. We were not able to confirm our hypothesis that *Fgf8* and *Pax9* would at least be partially downregulated in jervine-treated embryos. This might be due to the inability of the in situ technique to detect subtle quantitative differences, or it could indicate that other Shh-independent factors are required for competence of medial mandibular arch tissues to form the incisors.

Another line of evidence supporting a role for *Shh* in mandibular outgrowth comes from mutant studies. Mice that lack a functional *Shh* gene display an almost complete absence of craniofacial skeletal elements, despite a relatively normal appearance of the pharyngeal arches up to E9.5 (Chiang et al., 1996). These data again indicate that mandibular development is highly dependent upon Shh from E9.5 onwards. The authors suggest that the craniofacial abnormalities might be a secondary consequence of the severe midbrain and forebrain defects that were also found in these mutants. Although this may be the case for the nasal and maxillary structures, we deem it unlikely that mid- or forebrain can influence morphogenesis of the distant mandibular arch at E9.5. In addition, mouse embryos exposed to jervine at E7.5 frequently develop forebrain defects, but no mandibular defects (Omnell et al., 1990). The fact that the sensitive period for induction of lower jaw malformations by jervine is much later than that for induction of forebrain abnormalities suggests that the role of hedgehog signaling in development of the lower jaw is independent from its role in development of the forebrain.

The combined data presented above strongly support the notion that there is a causative link between the downregulation of *Shh* and abnormal mandibular morphogenesis in *Prx1*$^{-/-}$*Prx2*$^{-/-}$ mutants. In addition, these data reveal an unexpected role for Shh in the early establishment of the mandibular incisors, at a stage well before visible events that mark the initiation of tooth development.

A genetic network regulating mandibular morphogenesis

By analysis of patterns of BrdU labeling, we show that BrdU incorporation was reduced specifically in the medial-oral area of the mandibular arch in *Prx1*$^{-/-}$*Prx2*$^{-/-}$ mutant embryos. This indicates a reduction of cell proliferation in this area. Prx1 and Prx2 may either directly or indirectly regulate rates of cell proliferation in the mandibular arch. A likely explanation is that Prx1 and Prx2 regulate cell proliferation via Shh. In agreement with this is the observation that the area of reduced proliferation is directly underneath the epithelium showing reduced *Shh* expression. Shh has been shown to stimulate cell proliferation in a number of developmental contexts (see, for example, Wechsler-Reya and Scott, 1999; Jensen and Wallace, 1997), and it is therefore possible that its role in morphogenesis often depends on mitogenic activity. Although on the basis of cell proliferation patterns alone we cannot predict how morphogenesis will occur, we suggest that the observed

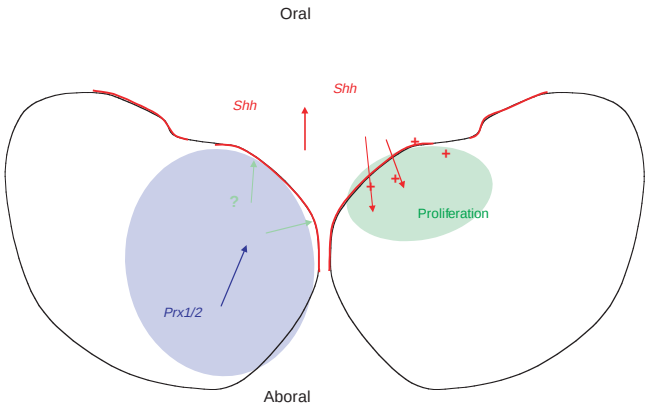

Fig. 7. Relationship between *Prx1*/*Prx2*, *Shh* and cell proliferation in the E10.5 mandibular arch. Prx1 and Prx2 in medial mandibular arch mesenchyme regulate the production of an unknown signaling factor (?). This factor signals to the oral epithelium and stimulates the expression of *Shh*. Shh signals back to the mesenchyme and stimulates cell proliferation.

reduction in cell proliferation leads to a reduction of medial tissue, and is causative for the observed shape changes in the mutant mandibular arch.

We propose a model that explains the observed abnormalities in the mandibular arch of *Prx1*$^{-/-}$*Prx2*$^{-/-}$ embryos (Fig. 7). According to this model, *Prx1* and *Prx2* expression in mandibular mesenchyme is required to stimulate the expression of *Shh* in the medial domain of the oral epithelium via a yet unknown intermediate. The Shh protein then promotes cell proliferation in part of the underlying mesenchyme, which is required for correct morphogenesis. In the *Prx1*$^{-/-}$*Prx2*$^{-/-}$ mutant, reduction of *Shh* expression leads to reduction of mesenchymal proliferation in the medial-oral region. This lack of proliferation causes a malformation of the mandibular processes such that the oral region develops in a more medial position, and the aboral region in a more lateral position (Fig. 2F,G). Consequently, the oral expression domains of *Dlx2*, *Alx3* and *Fgf8* shift medially, while the aboral domains of *Dlx2* and *Alx3* shift laterally. *Fgf8* expression in the medial region subsequently induces the formation of the medial incisor.

The occasional absence of both incisors in *Prx1*$^{-/-}$*Prx2*$^{-/-}$ mutants is not accounted for by this model. A possible explanation is suggested by the observation that exposure of embryos to jervine can lead to loss of the incisors. This indicates that a threshold level of Shh is required for incisor establishment. The level of Shh in the oral epithelium of *Prx1*$^{-/-}$*Prx2*$^{-/-}$ mutants may occasionally drop below this threshold, leading to loss of the incisor. Currently we understand little about how Shh enables around E9.5 the establishment of incisors. Our results suggest that Shh acts as a mitogen in the mandibular arch mesenchyme. Its downregulation may lead to insufficient expansion of mesenchymal tooth-germ precursor cells. In agreement with this are observations by Lu et al. (Lu et al., 1999), on independently created *Prx1*$^{-/-}$*Prx2*$^{-/-}$ mutants. They describe the presence of a single medial incisor in *Prx1*$^{-/-}$*Prx2*$^{+/-}$ mutants, and the absence of mandibular incisors in *Prx1*$^{-/-}$*Prx2*$^{-/-}$ mutants. However, they report the presence of a small incisor bud, that was arrested at the bud stage, in *Prx1*$^{-/-}$*Prx2*$^{-/-}$ mutants (Lu et al., 1999). We suggest that the initial tooth germ needs to have a minimum size in order to complete its development. One of the functions of Shh during mandibular development is then to ensure appropriate expansion of the tooth-germ precursor cells.

We are grateful to Willem Hage for assistance with confocal microscopy. We also thank Jeroen Charité for the use of the p(BH1100)$_4$-promoter/enhancer; Marie-José Goumans and Andrea Caricasole for help with immunohistochemistry; and Annemiek Beverdam, Jacqueline Deschamps and Ronald Plasterk for critically reading the manuscript. We would like to acknowledge Rolf Zeller and Aimée Zúñiga (Utrecht) for the suggestion to investigate the involvement of Shh. E. J. v. R. was partially supported by a grant from the Netherlands Organization for Scientific Research (NWO-ALW/STW).

REFERENCES

Bee, J. and Thorogood, P. (1980). The role of tissue interactions in the skeletogenic differentiation of avian neural crest cells. *Dev. Biol.* **78**, 47-62.
Charité, J., de Graaff, W., Vogels, R., Meijlink, F. and Deschamps, J. (1995). Regulation of the Hoxb-8 gene: synergism between multimerized cis-acting elements increases responsiveness to positional information. *Dev. Biol.* **171**, 294-305.
Chiang, C., Litingtung, Y., Lee, E., Young, K. W., Corden, J. L., Westphal, H. and Beachy, P. A. (1996). Cyclopia and defective axial patterning in mice lacking *Sonic hedgehog* gene function. *Nature* **383**, 407-413.
Cooper, M. K., Porter, J. A., Young, K. E. and Beachy, P. A. (1998). Teratogen-mediated inhibition of target tissue response to Shh signaling. *Science* **280**, 1603-1607.
Cserjesi, P., Lilly, B., Bryson, L., Wang, Y., Sassoon, D. A. and Olson, E. N. (1992). MHox: a mesodermally restricted homeodomain protein that binds an essential site in the muscle creatine kinase enhancer. *Development* **115**, 1087-1101.
Echelard, Y., Epstein, D. J., St. Jacques, B., Shen, L., Mohler, J., McMahon, J. A. and McMahon, A. P. (1993). *Sonic hedgehog*, a member of a family of putative signaling molecules, is implicated in the regulation of CNS polarity. *Cell* **75**, 1417-1430.
Ericson, J., Muhr, J., Piaczek, M., Lints, T., Jessell, T. M. and Edlund, T. (1995). Sonic hedgehog induces the differentiation of ventral forebrain neurons: a common signal for ventral patterning within the neural tube. *Cell* **81**, 747-756.
Goodrich, L. V., Johnson, R. L., Milenkovic, L., McMahon, J. A. and Scott, M. P. (1996). Conservation of the hedgehog/patched signaling pathway from flies to mice: induction of a mouse patched gene by Hedgehog. *Genes. Dev.* **10**, 301-312.
Goodrich, L. V., Jung, D., Higgins, K. M. and Scott, M. P. (1999). Overexpression of *ptc1* inhibits induction of *Shh* target genes and prevents normal patterning in the neural tube. *Dev. Biol.* **211**, 323-334.
Hall, B. K. (1980). Tissue interactions and the initiation of osteogenesis and chondrogenesis in the neural crest-derived mandibular skeleton of the embryonic mouse as seen in isolated murine tissues and in recombinations of murine and avian tissues. *J. Embryol. Exp. Morphol.* **58**, 251-264.
Helms, J. A., Kim, C. H., Hu, D., Minkoff, R., Thaller, C. and Eichele, G. (1997). *Sonic hedgehog* participates in craniofacial morphogenesis and is down-regulated by teratogenic doses of retinoic acid. *Dev. Biol.* **187**, 25-35.
Incardona, J. P., Gaffield, W., Kapur, R. P. and Roelink, H. (1998). The teratogenic *Veratrum* alkaloid cyclopamine inhibits Sonic hedgehog signal transduction. *Development* **125**, 3553-3562.
Jensen, A. M. and Wallace, V. A. (1997). Expression of *Sonic hedgehog* and its putative role as a precursor cell mitogen in the developing mouse retina. *Development* **124**, 363-371.
Johnson, R. L., Grenier, J. K. and Scott, M. P. (1995). *patched* overexpression alters wing disc size and pattern: transcriptional and post-transcriptional effects on *hedgehog* targets. *Development* **121**, 4161-4170.
Kern, M. J., Witte, D. P., Valerius, M. T., Aronow, B. J. and Potter, S. S. (1992). A novel murine homeobox gene isolated by a tissue specific PCR cloning strategy. *Nucleic Acids Res.* **20**, 5189-5195.
Kettunen, P. and Thesleff, I. (1998) Expression and function of FGFs-4, -8

and -9 suggest functional redundancy and repetitive use as epithelial signals during tooth morphogenesis. *Dev. Dyn.* **211**, 256-268.

Kollar, E. J. and Mina, M. (1991). Role of the early epithelium in the patterning of the teeth and Meckel's cartilage. *J. Craniofacial Genet. Dev. Biol.* **11**, 223-228.

Krauss, S., Concordet, J. P. and Ingham, P. W. (1993). A functionally conserved homolog of the Drosophila segment polarity gene *hh* is expressed in tissues with polarizing activity in zebrafish embryos. *Cell* **75**, 1431-1444.

Laufer, E., Nelson, C. E., Johnson, R. L., Morgan, B. A. and Tabin, C. (1994). Sonic hedgehog and Fgf-4 act through a signaling cascade and feedback loop to integrate growth and patterning of the developing limb bud. *Cell* **79**, 993-1003.

Leussink, B., Brouwer, A., El Khattabi, M., Poelmann, R. E., Gittenberger-de Groot, A. C. and Meijlink, F. (1995). Expression patterns of the paired-related homeobox genes *MHox/Prx1* and *S8/Prx2* suggest roles in development of the heart and the forebrain. *Mech. Dev.* **52**, 51-64.

Lu, M., Cheng, H., Kern, M. J., Potter, S. S., Tran, B., Diekwisch, T. G. H. and Martin, J. F. (1999). *prx-1* functions cooperatively with another *paired*-related homeobox gene, *prx-2*, to maintain cell fates within the craniofacial mesenchyme. *Development* **126**, 495-504.

Martin, J. F., Bradley, A. and Olson, E. N. (1995). The *paired*-like homeo box gene *MHox* is required for early events of skeletogenesis in multiple lineages. *Genes Dev.* 9, 1237-1249.

Mathews, M. B., Bernstein, R. M., Franza, B. R. Jr, Garrels, J. I. (1984). Identity of the proliferating cell nuclear antigen and cyclin. *Nature* **309**, 374-376.

Meijlink, F., Beverdam, A., Brouwer, A., Oosterveen, T. C. and ten Berge, D. (1999). Vertebrate aristaless-related genes. *Int. J. Dev. Biol.* **43**, 651-663.

Neubüser, A., Peters, H., Balling, R. and Martin, G. R. (1997). Antagonistic interactions between FGF and BMP signaling pathways: a mechanism for positioning the sites of tooth formation. *Cell* **90**, 247-255.

Niswander, L., Jeffrey, S., Martin, G. R. and Tickle, C. (1994). A positive feedback loop coordinates growth and patterning in the vertebrate limb. *Nature* **371**, 609-612.

Omnell, M. L., Sim, F. R. P., Keeler, R. F., Harne, L. C. and Brown, K. S. (1990). Expression of *Veratrum* alkaloid teratogenicity in the mouse. *Teratology* **42**, 105-119.

Opstelten, D. E., Vogels, R., Robert, B., Kalkhoven, E., Zwartkruis, F., de Laaf, L., Destrée, O. H., Deschamps, J., Lawson, K. A. and Meijlink, F. (1991). The mouse homeobox gene, *S8*, is expressed during embryogenesis predominantly in mesenchyme. *Mech. Dev.* **34**, 29-42.

Qiu, M., Bulfone, A., Ghattas, I., Meneses, J., Christensen, L., Sharpe, P. T., Presley, R., Pedersen, R. A. and Rubenstein, J. L. R. (1997). Role of the Dlx homeobox genes in proximdistal patterning of the branchial arches: mutations of Dlx-1, Dlx-2, and Dlx-1 and -2 alter morphogenesis of proximal skeletal and soft tissue structures derived from the first and second arch. *Dev. Biol.* **185**, 165-184.

Roessler, E., Belloni, E., Gaudenz, K., Jay, P., Berta, P., Scherer, S. W., Tsui, L and Muenke, M. (1996). Mutations in the human *Sonic Hedgehog* gene cause holoprosencephaly. *Nat. Genet.* **14**, 357-360.

ten Berge, D., Brouwer, A., El Bahi, S., Guénet, J., Robert, B. and Meijlink, F. (1998a). Mouse *Alx3*: an *aristaless*-like homeobox gene expressed during embryogenesis in ectomesenchyme and lateral plate mesoderm. *Dev. Biol.* **199**, 11-25.

ten Berge, D., Brouwer, A., Korving, J., Martin, J. F. and Meijlink, F. (1998b). *Prx1* and *Prx2* in skeletogenesis: roles in the craniofacial region, inner ear and limbs. *Development* **125**, 3831-3842.

Tucker, A. S., Yamada, G., Grigoriou, M., Pachnis, V. and Sharpe, P. T. (1999). Fgf-8 determines rostral-caudal polarity in the first branchial arch. *Development* **126**, 51-61.

van Raaij, E., Van Raaij, E. J., ten Berge, D., Hage, W. J., Brouwer, A., Meijlink, F. M., Maintz, J. B. A., Verbeek, F. J. (2001). Automated topographical cell proliferation analysis. *Cytometry* (in press).

Wall, N. A. and Hogan, B. L. (1995). Expression of bone morphogenetic protein-4 (BMP-4), bone morphogenetic protein-7 (BMP-7), fibroblast growth factor-8 (FGF-8) and sonic hedgehog (SHH) during branchial arch development in the chick. *Mech. Dev.* **53**, 383-392.

Wechsler-Reya, R. J. and Scott, M. P. (1999). Control of neuronal precursor proliferation in the cerebellum by Sonic hedgehog. *Neuron* **22**, 103-114.